

Efficient Non-Resonant Microwave Absorption in Thin Cylindrical Targets: Experimental Evidence

A. Akhmeteli*
LTASolid Inc.
 10616 Meadowglen Ln 2708,
 Houston, TX 77042, USA

N. G. Kokodiy,[†] B.V. Safronov, V.P. Balkashin, and I.A. Priz
Kharkov National University
 Ukraine, Kharkov, Svobody sqw., 4

A. Tarasevitch
University of Duisburg-Essen,
Institute of Experimental Physics
 Lotharstr. 1, 47048 Duisburg, Germany
 (Dated: January 22, 2022)

Significant (up to 6%) absorption of microwave power focused on a thin fiber (the diameter is three orders of magnitude less than the wavelength) by an ellipsoidal reflector is demonstrated experimentally. This new physical effect can be used in numerous applications, for example, for efficient heating of nanotubes by laser beams.

PACS numbers: 41.20.-q, 42.25.Fx, 52.50.Jm, 81.07.De

I. INTRODUCTION

A theoretical possibility of non-resonant, fast, and efficient heating of extremely thin conducting cylindrical targets by broad electromagnetic beams was described in Ref. [1] (see also the sections on the "transverse geometry" in Refs. [2, 3] and references there). The diameter of the cylinder can be orders of magnitude smaller than the wavelength of the electromagnetic radiation. Efficient heating takes place for converging axisymmetric cylindrical waves (under some limitations on the real part of the complex permittivity of the cylinder) if the diameter of the cylinder and the skin-depth are of the same order of magnitude and the electric field in the wave is directed along the common axis of the cylinder and the wave (see the exact conditions in Refs. [2, 3]). This possibility can be used to create high energy density states for such applications as pumping of active media of short-wavelength lasers and nuclear fusion. For example, an exciting possibility of efficient heating of nanotubes by femtosecond laser pulses is discussed in Ref. [3].

In this work we present the first experimental confirmation of the predictions of Refs. [1–3]) (some preliminary results for a somewhat problematic configuration were presented in Ref. [4]). In our experiment, a thin fiber (with a diameter three orders of magnitude smaller than the wavelength) absorbed up to 6% of the microwave power focused on the fiber with an ellipsoidal reflector.

Work [1–3] had important predecessors. Shevchenko (Ref. [5]) derived optimal conditions of absorption of a plane electromagnetic wave in a thin conducting wire that are similar to the conditions of Refs. [1–3]. However, the possibility of efficient heating of a thin wire or fiber, when the power absorbed in a thin conducting wire or fiber is comparable to the power in the incident wave, was not noticed in work [5], as heating by a plane wave is very inefficient. On the other hand, the transverse geometry of Refs. [1–3] (heating by a converging axisymmetric cylindrical wave) was also considered, e.g., in Ref. [6], but that work only contains resonant conditions of heating, which are difficult to use for practical plasma heating.

The results of Ref. [5] found experimental confirmation in Ref. [7]. The experimental results of Ref. [7], motivated by the theoretical results for a plane wave, were obtained for absorption of microwave H_{01} mode at the output of a waveguide, and heating efficiency was not assessed. In the present experiment, we demonstrate efficient heating of a thin fiber by an electromagnetic beam in free space. The experimental results are in satisfactory agreement (typically up to a factor of 2) with theoretical computations.

II. THE EXPERIMENTAL SETUP

The experimental setup is shown schematically in Fig. 1. A thin wire or fiber is placed in focus F_1 of the ellipsoidal reflector. The internal surface of the reflector is a part of an ellipsoid of revolution defined by the equation:

$$\frac{x^2}{a^2} + \frac{y^2 + z^2}{b^2} = 1, \quad (1)$$

*Electronic address: akhmeteli@ltasolid.com;
 URL: <http://www.akhmeteli.org>

[†]Electronic address: kokodiy.n.g@gmail.com

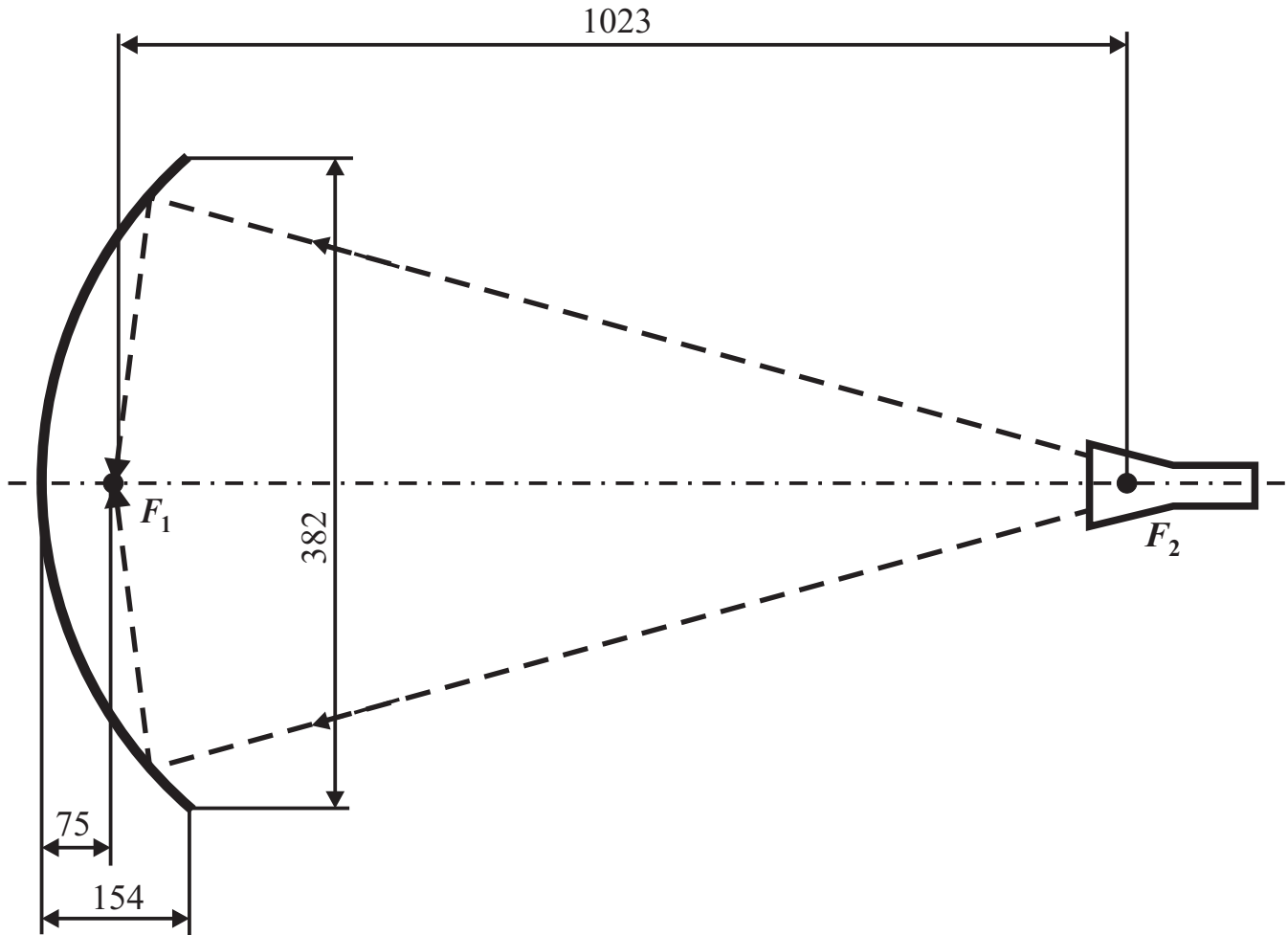


FIG. 1: The experimental setup (not to scale)

where $a \approx 586$ mm is the major semiaxis and $b \approx 287$ mm is the minor semiaxis of the relevant ellipse. The distance between the foci F_1 and F_2 is approximately 1023 mm. The dimensions of the reflector and the position of focus F_1 inside the reflector are shown in Fig. 1. A horn with aperture 31×22 mm² and length 130 mm is placed in focus F_2 (the distance between the horn aperture and the focus is 65 mm). The wide side of the horn is horizontal. The horn is connected to a waveguide with dimensions 7.2×3.4 mm² with mode H_{10} . The frequency of the electromagnetic radiation varied from 24.5 GHz to 39 GHz, and the power varied from 20 mW to 61 mW. Typically, most of the power is collected by the reflector and focused in focus F_1 .

III. MEASUREMENT AND COMPUTATION METHODS

The wire or fiber in the focus is heated by the radiation, and the initial electrical resistance of the wire/fiber R_0 changes by ΔR . The average wire/fiber temperature

increase ΔT corresponding to ΔR was calculated as

$$\Delta T = \frac{\Delta R}{\alpha_r R_0}, \quad (2)$$

where α_r is the temperature coefficient of resistance.

On the other hand, the steady state wire/fiber temperature increase depends on the absorbed power P_a and the conditions of heat exchange with the environment [7]:

$$\Delta T = \frac{P_a}{a_p L}, \quad (3)$$

where L is the length of the wire/fiber and a_p is the linear heat exchange coefficient. For the carbon fiber of diameter 11μ , this coefficient was measured as follows. For a direct current in the fiber, the Joule power was calculated based on the measurements of the current and the voltage, and the temperature increase was calculated based on the measured change of the fiber resistivity. The value of the coefficient differed slightly for a vertical and horizontal fiber: 0.017 W/(m-deg) and 0.019 W/(m-deg), respectively. For the platinum wire of diameter 3.5μ , the following values obtained by N. G. Kokodiy and A. O.

Pak (private communication) were used for the vertical and horizontal orientation of the wire: 0.023 W/(m-deg) and 0.026 W/(m-deg), respectively.

It follows from Eqs. (2,3) that

$$P_a = \frac{\alpha_p L \Delta R}{\alpha_r R_0}. \quad (4)$$

Therefore, the efficiency of absorption of microwave power in the wire/fiber equals:

$$K = \frac{P_a}{P} = \frac{\alpha_p L \Delta R}{\alpha_r P R_0}, \quad (5)$$

where P is the power in the microwave beam.

In the experiment, microwave absorption in two targets was studied: 1) a platinum wire of diameter 3.5 micron and length ≈ 25 mm, and 2) a carbon fiber [8] of diameter 11 micron and length ≈ 30 mm. For the platinum wire, a tabular value $\alpha_r = 0.004 \text{ deg}^{-1}$ was used, and for the carbon fiber, the value $\alpha_r = 0.00021 \text{ deg}^{-1}$ was found experimentally based on the current-voltage curve.

The experimental results were compared with the results of computations. The feed horn fields (incident on

the reflector) were computed using the following formulas for the far zone of a pyramidal horn [9].

If the origin is in the center of the horn aperture, and axes x' , y' , and z' are directed parallel to the broad sides of the horn, parallel to the narrow sides of the horn, and along the horn axis, respectively, the radial distance, inclination angle, and azimuthal angle of the relevant spherical system of coordinates are r , θ , and φ , respectively. The components of the magnetic field in the far zone are

$$H_r(r, \theta, \varphi) = 0,$$

$$H_\theta(r, \theta, \varphi) = -\frac{ik \exp(-ikr)}{4\pi r} \frac{E_0}{\eta} I_1 I_2 \cos(\varphi)(1 + \cos(\theta)),$$

$$H_\varphi(r, \theta, \varphi) = \frac{ik \exp(-ikr)}{4\pi r} \frac{E_0}{\eta} I_1 I_2 \sin(\varphi)(1 + \cos(\theta)), \quad (6)$$

where the temporal dependence factor $\exp(i\omega t)$ is omitted, E_0 is the amplitude of the electric field in the center of the horn aperture for the dominant mode,

$$I_1 = \frac{1}{2} \sqrt{\frac{\pi \rho_2}{k}} \times (\exp(ik_x'^2 \rho_2 / 2k) (C(t_2') - C(t_1') - i(S(t_2') - S(t_1'))) + \exp(ik_x''^2 \rho_2 / 2k) (C(t_2'') - C(t_1'') - i(S(t_2'') - S(t_1'')))),$$

$$I_2 = \sqrt{\frac{\pi \rho_1}{k}} \exp(ik_y^2 \rho_2 / 2k) (C(t_2) - C(t_1) - i(S(t_2) - S(t_1))), \quad (7)$$

$C(x)$ and $S(x)$ are the cosine and sine Fresnel integrals, respectively, ρ_1 is the distance from the horn aperture plane to the line of intersection of two opposite broad faces of the horn pyramid, ρ_2 is the distance from the horn aperture plane to the line of intersection of two op-

posite narrow faces of the horn pyramid,

$$t_1' = \sqrt{\frac{1}{\pi k \rho_2}} \left(-\frac{ka_1}{2} - k_x' \rho_2 \right),$$

$$t_2' = \sqrt{\frac{1}{\pi k \rho_2}} \left(+\frac{ka_1}{2} - k_x' \rho_2 \right),$$

$$k_x' = k \sin(\theta) \cos(\varphi) + \frac{\pi}{a_1},$$

$$t_1'' = \sqrt{\frac{1}{\pi k \rho_2}} \left(-\frac{ka_1}{2} - k_x'' \rho_2 \right),$$

$$t_2'' = \sqrt{\frac{1}{\pi k \rho_2}} \left(+\frac{ka_1}{2} - k_x'' \rho_2 \right),$$

$$k_x'' = k \sin(\theta) \cos(\varphi) - \frac{\pi}{a_1},$$

$$t_1 = \sqrt{\frac{1}{\pi k \rho_1}} \left(-\frac{kb_1}{2} - k_y \rho_1 \right),$$

$$t_2 = \sqrt{\frac{1}{\pi k \rho_1}} \left(\frac{kb_1}{2} - k_y \rho_1 \right),$$

$$k_y = k \sin(\theta) \sin(\varphi),$$

(8)

a_1 and b_1 are the lengths of the wide and the narrow sides of the horn aperture, respectively, and η is the intrinsic impedance of the media (air).

The reflected fields for the ellipsoidal reflector were estimated using methods of physical optics [10], as the radii of curvature of the reflector are much greater than the wavelength everywhere. The reflected electric field \mathbf{E}_s in a field point is calculated using the following formula (Ref. [10]):

$$\mathbf{E}_s = \frac{1}{2\pi i \omega \varepsilon} \times \int_{S_0} ((\mathbf{n} \times \mathbf{H}_i) \cdot \nabla (\nabla \Psi) + k^2 (\mathbf{n} \times \mathbf{H}_i) \Psi) dS, \quad (9)$$

where $\Psi = \exp(-ikR/R)$, R is the distance from the field point to the element of area dS on the reflector, gradient operations in the integrand are referred to the field point as an origin, \mathbf{n} is the normal to the reflector surface, S_0 is the geometrically illuminated surface of the reflector, components of the incident magnetic field \mathbf{H}_i are defined by Eq. (6), ε is the media permittivity.

Absorption of the reflected field of the ellipsoidal reflector in the wire/fiber in the focus of the reflector was computed using the rigorous solution of the problem of diffraction of electromagnetic field on a homogeneous cylinder (Ref. [11]), which has a simpler form in the case of axisymmetrical field (non-axisymmetrical field is not efficiently absorbed in a very thin cylinder). The field incident on the cylinder (wire/fiber) is described by the electric Hertz vector (Ref. [12]) $\mathbf{\Pi}(\rho, \varphi, z) = \{0, 0, \Pi(\rho, \varphi, z)\}$. We use a cylindrical coordinate system ρ, φ, z , where axis z coincides with the axis of the cylinder. We do not use the magnetic Hertz vector as the relevant TE field is not efficiently absorbed in a thin cylinder. Therefore, the reflected field of the ellipsoidal reflector (which is the incident field for the cylinder) is defined by the following expansion of the z -component of the electric Hertz vector into cylindrical waves (Ref. [12]):

$$\Pi(\rho, \varphi, z) = \int d\gamma \alpha(\gamma) J_0(\lambda_1(\gamma)\rho) \exp(i\gamma z), \quad (10)$$

where the limits of integration are $-\infty$ and ∞ , $J_n(x)$ is the Bessel function of order n , $\lambda_1^2(\gamma) = \varepsilon_1 k_0^2 - \gamma^2$ (it is assumed that magnetic permeabilities of air and the cylinder, μ_1 and μ_2 , equal 1), $\varepsilon_1 \approx 1$ is the electric permittivity of air, $k_0 = \omega/c$ is the wave vector in vacuum, $\omega = 2\pi\nu$ is the frequency of the electromagnetic field (the factor $\exp(-\omega t)$ is omitted). Function $\alpha(\gamma)$ can be defined as follows. The z -component of the incident electric field corresponding to Eq. (10) can be written as follows:

$$E_z(\rho, \varphi, z) = \int d\gamma \alpha(\gamma) \frac{\lambda_1^2(\gamma)}{\varepsilon_1} J_0(\lambda_1(\gamma)\rho) \exp(i\gamma z), \quad (11)$$

so

$$\alpha(\gamma) \lambda_1^2(\gamma) = E_z(\gamma) = \frac{1}{2\pi} \int dz E_z(z) \exp(i\gamma z), \quad (12)$$

where $E_z(z)$ is the z -component of the incident electric field on the axis of the cylinder (where $\rho = 0$ and $J_0(\lambda_1(\gamma)\rho) = 1$), computed using Eq. (9), and $E_z(\gamma)$ is its Fourier transform. Eq. (11) correctly describes the z -component of the incident electric field in the vicinity of the axis, although Eq. (10) does not include the TE-field and non-axisymmetrical field, which are not efficiently absorbed in the thin cylinder.

The z -component of the electrical Hertz vector of the field refracted in the cylinder can be calculated using the rigorous solution of the problem of diffraction of electromagnetic field on a homogeneous cylinder (Ref. [2, 11]):

$$u_2(\rho, \varphi, z) = \int d\gamma a_2(\gamma) J_0(\lambda_2(\gamma)\rho) \exp(i\gamma z), \quad (13)$$

where

$$a_2(\gamma) = \frac{\alpha(\gamma) \frac{\varepsilon_2}{\varepsilon_1} \frac{1}{J_0(p_2(\gamma))} \frac{-2i}{\pi p_2^2(\gamma) H_0^{(1)}(p_1(\gamma))}}{-\left(\frac{1}{p_1(\gamma)} \frac{H_0^{(1)'}(p_1(\gamma))}{H_0^{(1)}(p_1(\gamma))} - \frac{1}{p_2(\gamma)} \frac{\varepsilon_2}{\varepsilon_1} \frac{J_0'(p_2(\gamma))}{J_0(p_2(\gamma))}\right)} = \frac{\alpha(\gamma) \varepsilon_2 \frac{1}{J_0(p_2(\gamma))} \frac{2i}{\pi p_2^2(\gamma) H_0^{(1)}(p_1(\gamma))}}{\frac{1}{p_2(\gamma)} \varepsilon_2 \frac{J_1(p_2(\gamma))}{J_0(p_2(\gamma))} - \frac{1}{p_1(\gamma)} \frac{H_1^{(1)}(p_1(\gamma))}{H_0^{(1)}(p_1(\gamma))}}, \quad (14)$$

as $\varepsilon_1 \approx 1$ and, for example, $H_0^{(1)' } = -H_1^{(1)}$, $\varepsilon_2 = \varepsilon = \varepsilon' + 4\pi i\sigma/\omega$ is the complex electric permittivity of the cylinder, ε' is the real part of the permittivity, σ is the conductivity of the cylinder, $p_1(\gamma) = \lambda_1(\gamma)a$, $p_2(\gamma) = \lambda_2(\gamma)a$, a is the radius of the cylinder, $H_n^{(1)}(x)$ is the Hankel function, $\lambda_2^2(\gamma) = \varepsilon_2 k_0^2 - \gamma^2$.

The averaged ρ -component of the Poynting vector at the surface of the cylinder equals

$$\frac{1}{2} \frac{c}{4\pi} \Re \left((\mathbf{E}(a, \varphi, z) \times \mathbf{H}^*(a, \varphi, z))_\rho \right) = -\frac{1}{2} \frac{c}{4\pi} \Re (E_z(a, \varphi, z) H_\varphi^*(a, \varphi, z)), \quad (15)$$

as $H_z(a, \varphi, z) = 0$.

The total power absorbed in the cylinder W equals

$$-2\pi a \int dz \left(-\frac{1}{2} \frac{c}{4\pi} \right) \Re (E_z(a, \varphi, z) H_\varphi^*(a, \varphi, z)) = \frac{ac}{4\pi} \int dz \Re (E_z(a, \varphi, z) H_\varphi^*(a, \varphi, z)) \quad (16)$$

(an extra minus sign is introduced as positive ρ -component of the Poynting vector corresponds to energy flow out of the cylinder, and we are interested in the absorbed power.) Although the limits of integration are $-\infty$ and ∞ , the reflected fields of the ellipsoidal reflector are negligible beyond the focal area. The components of the electric and magnetic field for the electric Hertz vector of Eq. (13) equal

$$\begin{aligned}
E_z(a, \varphi, z) &= \int d\gamma a_2(\gamma) \exp(i\gamma z) \frac{\lambda_2^2(\gamma)}{\epsilon_2} J_0(p_2(\gamma)), \\
H_\varphi^*(a, \varphi, z) &= \int d\gamma' a_2^*(\gamma') \exp(-i\gamma' z) (-ik_0) \lambda_2^*(\gamma') J_0'(p_2(\gamma')),
\end{aligned} \tag{17}$$

so

$$\begin{aligned}
& \int dz E_z(a, \varphi, z) H_\varphi^*(a, \varphi, z) = \\
&= \int dz \int d\gamma a_2(\gamma) \exp(i\gamma z) \frac{\lambda_2^2(\gamma)}{\epsilon_2} J_0(p_2(\gamma)) \int d\gamma' a_2^*(\gamma') \exp(-i\gamma' z) (-ik_0) \lambda_2^*(\gamma') J_0'(p_2(\gamma')) = \\
&= \int \int d\gamma d\gamma' a_2(\gamma) a_2^*(\gamma') \frac{\lambda_2^2(\gamma)}{\epsilon_2} (-ik_0) \lambda_2^*(\gamma') J_0(p_2(\gamma)) J_0'(p_2(\gamma')) \int dz \exp(i\gamma z) \exp(-i\gamma' z) = \\
&= \int \int d\gamma d\gamma' a_2(\gamma) a_2^*(\gamma') \frac{\lambda_2^2(\gamma)}{\epsilon_2} (-ik_0) \lambda_2^*(\gamma') J_0(p_2(\gamma)) J_0'(p_2(\gamma')) 2\pi \delta(\gamma - \gamma') = \\
&= 2\pi \int d\gamma a_2(\gamma) a_2^*(\gamma) \lambda_2^2(\gamma) \lambda_2^*(\gamma) \frac{-ik_0}{\epsilon_2} J_0(p_2(\gamma)) J_0'(p_2(\gamma)),
\end{aligned} \tag{18}$$

and

$$\begin{aligned}
& \Re \left(\frac{-ik_0}{\epsilon_2 \lambda_2^*(\gamma)} J_0(p_2(\gamma)) J_0'(p_2(\gamma)) \right) = \\
&= \Im \left(\frac{k_0}{\epsilon_2 \lambda_2^*(\gamma)} J_0(p_2(\gamma)) J_0'(p_2(\gamma)) \right) = \\
&= k_0 J_0(p_2(\gamma)) J_0'(p_2(\gamma)) \Im \left(\frac{1}{\epsilon_2 \lambda_2^*(\gamma)} \frac{J_0'(p_2(\gamma))}{J_0(p_2(\gamma))} \right) = \\
&= -k_0 J_0(p_2(\gamma)) J_0'(p_2(\gamma)) \Im \left(\frac{1}{\epsilon_2^* \lambda_2(\gamma)} \frac{J_0'(p_2(\gamma))}{J_0(p_2(\gamma))} \right). \tag{19}
\end{aligned}$$

Therefore, Eq. (16) can be rewritten as follows:

$$\begin{aligned}
W &= \frac{ac}{4} 2\pi \int d\gamma |a_2(\gamma) \lambda_2^2(\gamma) J_0(p_2(\gamma))|^2 (-k_0) \Im \left(\frac{1}{\epsilon_2^* \lambda_2(\gamma)} \frac{J_0'(p_2(\gamma))}{J_0(p_2(\gamma))} \right) = \\
&= \frac{k_0 ac}{4} 2\pi \int d\gamma |a_2(\gamma) \lambda_2^2(\gamma) J_0(p_2(\gamma))|^2 \Im \left(\frac{1}{\epsilon_2^* \lambda_2(\gamma)} \frac{J_1(p_2(\gamma))}{J_0(p_2(\gamma))} \right),
\end{aligned} \tag{20}$$

as $J_0'(x) = -J_1(x)$.

The radiated power of the pyramidal horn antenna (in the Gaussian system of units) equals [9]

$$W_0 = \frac{1}{4} \frac{c}{4\pi} a_1 b_1 E_0^2, \tag{21}$$

where a_1 and b_1 are the dimensions of the horn aperture and E_0 is the amplitude of the electric field in the center of the aperture. Therefore, the heating efficiency (the part of the radiated power that is absorbed in the cylinder) equals

$$\frac{W}{W_0} = \frac{8\pi^2 k_0 a \int d\gamma |a_2(\gamma) \lambda_2^2(\gamma) J_0(p_2(\gamma))|^2 \Im \left(\frac{1}{\epsilon_2^* \lambda_2(\gamma)} \frac{J_1(p_2(\gamma))}{J_0(p_2(\gamma))} \right)}{a_1 b_1 E_0^2}. \tag{22}$$

The following values of resistivity were used for the platinum wire and the carbon fiber, respectively: 0.106

$\mu\text{Ohm-m}$ and $13 \mu\text{Ohm-m}$.

While some manufacturer's data (Ref. [8]) were used in computations for the carbon fiber, the experimental data for the specific fiber were somewhat different. For example, the fiber diameter was measured using diffraction of a broad laser beam on the fiber, and the measured value was 10.1 ± 0.5 micron, rather than 13 micron. The fiber resistivity was determined using measurements of the fiber resistance and dimensions. The value of resistivity was $16 \pm 2 \mu\text{Ohm-m}$, rather than $13 \mu\text{Ohm-m}$. Using these parameters in computations did not result in significant modifications. For example, the part of power absorbed in the fiber changes from 9.7% to 10.4% at 39 GHz. The computed absorbed power changed insignificantly when the value of the real part of the complex electric permittivity of the fiber changed, e.g., from -1 to 5.

IV. EXPERIMENTAL AND THEORETICAL RESULTS

In Fig. 2, the dependence of absorption of electromagnetic power in the platinum wire on the frequency is shown. This case is not optimal for target heating, so only about 1% of the beam power is absorbed in the wire.

The experimental values are in good agreement with the theoretical ones. The test point scattering is caused by environmental factors. The wire is heated just by 1° or less, so air flows can significantly influence the results.

In Fig. 3, the same dependence is shown for the carbon fiber. In this case, significantly more power is absorbed – up to 6%. The experimental values are less than the theoretical ones, but the agreement seems satisfactory. Two experimental curves are given in the figure. The blue line represents the results for the case where the reflector was covered by a sheet of polystyrene foam to decrease air flows. The foam refraction index is close to unity, so microwave reflection coefficient for normal incidence is of the order of 0.1%. Therefore, the polystyrene foam sheet has very little effect on microwave propagation.

The discrepancy between theory and experiment may be due to inaccuracies of the fiber positioning or to a discrepancy between conductivity for direct current and for microwave frequencies.

To assess the effect of microwave field polarization on absorption in the fiber, the experiment was conducted for a horizontal orientation of the fiber, when the electric field is orthogonal to the wire. Within our approx-

imations, the theoretical absorption efficiency is zero in this case. The experimental values (less than 0.4%) were much less than for the other polarization, and the specific experimental values were not very reliable, as the fiber resistance changes were comparable to instrument error.

Absorption in the cylindrical target can be significantly greater for an axisymmetric converging cylindrical wave incident on the target. In this case, up to 40% of the incident power can be absorbed in the carbon fiber (see Fig. 4).

The absorption in the platinum wire is significantly less – about 4%.

The increase of absorption with frequency in our experiment probably can be explained as follows: for higher frequency, the horn pattern is more narrow, so the reflector gathers more power.

In this experiment, the absorption is relatively modest – about 6% for the carbon fiber. This is due to the selected configuration. As continuous wave was used in the experiment, care was taken to exclude a possibility of multi-path heating of the target. Electromagnetic radiation reflected from the wire and then from the reflector would be directed to the other focus of the reflector. The absorption efficiency is proportional to the square of the angle from which the incident power is directed on the target. In our experiment, this angle is significantly less than 360° (about 200°), so the efficiency is at least 3 times less than for the axisymmetrical cylindrical wave. However, in fast heating applications, the target can be irradiated from all directions, so higher efficiency can be achieved.

V. CONCLUSION

The results of the experiment confirm the feasibility of efficient heating of thin cylindrical targets with electromagnetic radiation with wavelength (and, consequently, the dimensions of the focal area) several orders of magnitude greater than the diameter of the target. To this end, it is necessary to create an incident field with a high axisymmetric content (with respect to the axis of the target) and proper polarization, and there needs to be a match between the diameter of the target, its conductivity, and the wavelength. However, the conditions of efficient heating are non-resonant and therefore very promising for numerous applications. The heating efficiency of tens percent can be achieved for very thin targets.

[1] A. M. Akhmeteli, in *III Inter-Republican Seminar 'Physics of Fast Processes'*, Grodno (1992), p. 4.

[2] A. Akhmeteli, physics/0405091.

[3] A. Akhmeteli, physics/0611169.

[4] A. Akhmeteli, N. G. Kokodiy, B. Safronov, V. Balkashin, I. Priz, and A. Tarasevitch, physics/1107.5921.

[5] V. V. Shevchenko, Soviet Journal of Communications Technology and Electronics **37(6)**, 121 (1992).

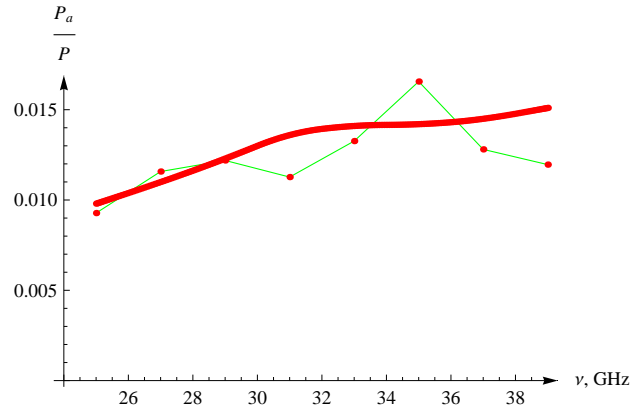


FIG. 2: Absorption of microwave radiation by a platinum wire in the focus of the reflector. Red line – theoretical curve; green line – experimental data.

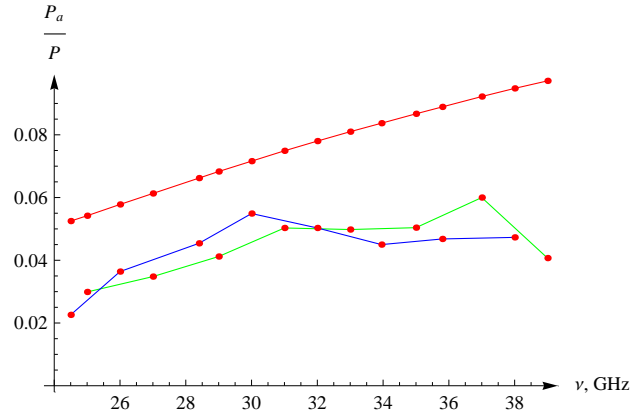


FIG. 3: Absorption of microwave radiation by a carbon fiber in the focus of the reflector. Red line – theoretical curve; green and blue lines – experimental data.

- [6] A. A. Zharov and T. M. Zaboronkova, Soviet Journal of Plasma Physics **9**, 580 (1983).
 [7] V. M. Kuz'michev, N. G. Kokodii, B. V. Safronov, and V. P. Balkashin, J. Commun. Technol. Electron. **48**, 1240 (2003).
 [8] Cytec, www.cytec.com/engineered-materials/products/Datasheets/P-25_RevA7-12-06.pdf.

- [9] C. A. Balanis, *Antenna Theory, 3rd ed.* (Wiley, 2005).
 [10] S. Silver, ed., *Microwave Antenna Theory and Design* (P. Peregrinus, 1984).
 [11] J. R. Wait, Can. Journ. of Phys. **33**, 189 (1955).
 [12] J. A. Stratton, *Electromagnetic Theory* (IEEE-Wiley, 2007).

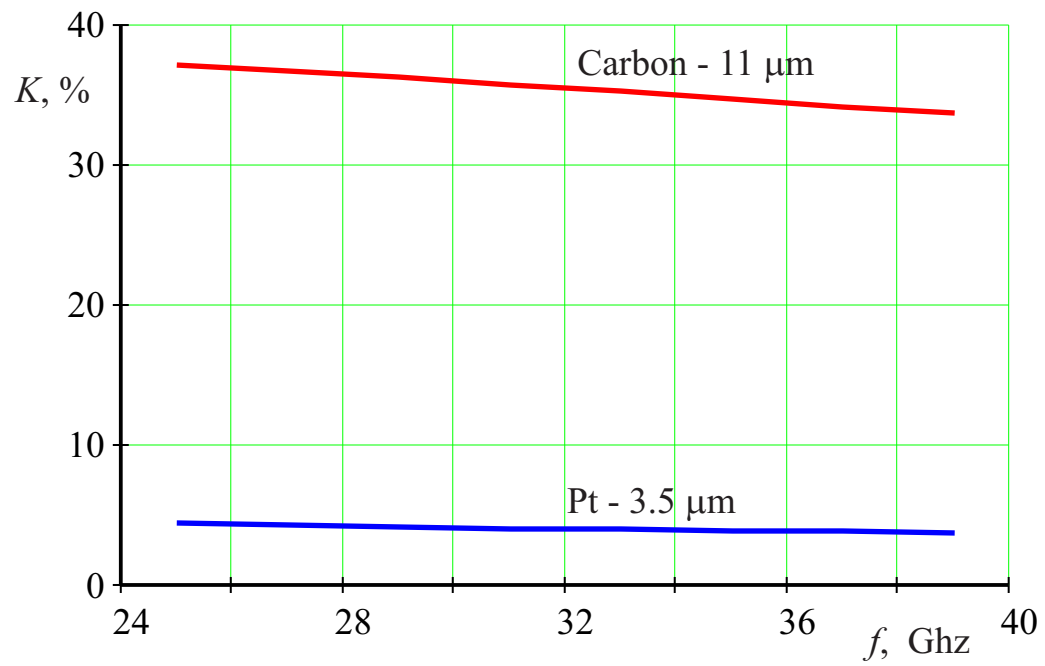


FIG. 4: Absorption of an axisymmetric converging cylindrical wave by a thin wire/fiber